X-612-65-482

TMX-55404

A MODEL EQUATORIAL ELECTROJET

BY
MASAHISA SUGIURA
JOSEPH C. CAIN

NOVEMBER 1965

GODDARD SPACE FLIGHT CENTER
GREENBELT, MARYLAND

A MODEL EQUATORIAL ELECTROJET

by

Masahisa Sugiura

and

Joseph C. Cain

NASA-Goddard Space Flight Center

Greenbelt, Md.

Abstract

The cross-sectional profile of the equatorial electrojet is determined for various longitudes along the dip equator, using a set of 48 Gauss coefficients for the earth's magnetic field. The electrojet profile is found to vary appreciably with longitude due to the asymmetry of the magnetic field. To demonstrate the longitudinal variation of the electrojet the profiles for longitudes 80° E (for India) and 280° E (for Peru) are shown. The maximum current density in the electrojet for the latter longitude is found to be much greater than that for the former longitude. Also the width of the electrojet is greater at 280° E than at 80° E. The magnetic field produced by the electrojet is computed for various longitudes along the dip equator and also for the locations of six magnetic observatories near the dip equator. The theoretically expected field changes are qualitatively in agreement with the observed values for these observatories. The average electron drift velocity in the electrojet is estimated; over Peru this velocity reaches a few km/sec during a sunspot maximum period at the height of the peak of the electrojet. This value is considerably higher than earlier estimates and is well above the critical electron velocity, i.e., the ion thermal velocity, above which the two-stream instability can occur.

Introduction

The recent rocket explorations of the equatorial electrojet in India (Maynard and Cahill, 1965a) and off the coast of Peru (Davis et al., 1965; Maynard and Cahill, 1965b) have stimulated general interest in this subject, and it seems timely to present a model electrojet with which the new measurements may be compared. The magnetic observations made in the equatorial regions at ground level have been discussed extensively (Onwumechilli, 1959a, 1959b; Osborne, 1962a, 1962b, 1963; Forbush and Casaverde, 1961). The model presented here is based on a model atmosphere described below and on the magnetic field configuration determined with the 48 Gauss coefficients given by Jensen and Cain (1962). These coefficients were chosen as being the most accurate available at the time this work was begun. A recalculation made with a more recent model (Hendricks and Cain, 1966) has shown that changes in the final results are sufficiently small that the conclusions drawn in this paper are not altered.

Assuming that the physical quantities of the ionosphere are the same everywhere along the dip equator except for the differences arising from the asymmetry of the earth's permanent magnetic field, the cross-sectional profile of the electrojet is determined for different longitudes. In particular, two such profiles, one for longitude 80°E for India and another for longitude 280°E for Peru, are presented. Using such profiles the magnitude of the magnetic field due to the electrojet as observed at ground level is computed as a function of longitude. The longitude variation so obtained is shown to be in fair agreement with the observations at several equatorial observatories.

The average electron drift velocity in the electrojet is estimated, and is shown to be well above the threshold velocity for the two-stream instability discussed by Farley (1963a, 1963b) and Buneman (1963).

Conductivity profile

We take a rectangular coordinate system (x, y, z) such that: the x-y plane coincides with the ground with the positive z axis pointing upward; the y axis is along the dip equator its positive direction being eastward; the x axis is directed south. The primary electric field is assumed to be static and parallel to the y axis; we denote this field by E_y. If we further assume that the vertical Hall current is entirely inhibited by the (vertical) polarization of the medium, this polarization field E_z is given by

$$E_z = [\sigma_2/(\sigma_o \tan^2 I + \sigma_1)]\, E_y$$

where σ_o, σ_1, and σ_2 are the direct, the Pedersen, and the Hall conductivity, respectively, and where I is the magnetic dip (Hirono, 1952; Baker and Martyn, 1953). Thus at the dip equator, where I = 0, the vertical polarization field is σ_2/σ_1 times the original horizontal field. In Figure 1 the ratio σ_2/σ_1 is plotted against height. (The ionospheric parameters used for the calculation of the conductivity elements are given in the Appendix.) In the region near 100 km level σ_2/σ_1 is extremely large, being 20 to 30. It is essentially this large vertical polarization field that dirves the electrojet. The sum of the Pedersen current $\sigma_1 E_y$ and the Hall current $\sigma_2 E_z$ is the total electrojet current. At the dip equator this is $\sigma_3 E_y$, where $\sigma_3 = \sigma_1 + \sigma_2^2/\sigma_1$; σ_3 is called the Cowling conductivity.

We denote the effective conductivity in the y direction by σ_{yy}, where

$$\sigma_{yy} = \sigma_1 + \sigma_2^2/(\sigma_o \tan^2 I + \sigma_1)$$

Since the electric field E_y is assumed to be uniform, the cross-sectional profile of σ_{yy} in the x-z plane gives the corresponding profile of the relative current density. The ionospheric parameters are taken to be functions of z alone; while the magnetic field as determined from the 48 Gauss coefficients varies with longitude along the dip equator. It is only the latter that generates the longitudinal variation of the electrojet profile. The electron density distribution at noon is not likely to be the same everywhere along the dip equator, but what we intend to show here is the effect of the nonuniformity of the magnetic field along the dip equator, separating this from other possible effects. We make an idealization that the primary electrostatic field is assumed to be uniform and parallel to the dip equator. The exact electric field distribution can be determined only if the wind pattern and the distributions of the electron density and other ionospheric quantities are completely known all over the world. Without a complete knowledge of these factors we have to rely on known properties of the magnetic variation Sq and of the associated electric field theoretically deduced. The general direction of the electric field in midday in the equatorial region as inferred by the dynamo theory is approximately eastward (Maeda, 1955). The characteristics of Sq are known to be similar along the lines of equal dip, and near noon the Sq current in low latitudes appears to flow nearly parallel to the dip equator (Price and Wilkins, 1963). Thus

for an idealized model the assumption that the primary electric field is parallel to the dip equator seems to be appropriate.

Figures 2 and 3 show contours of equal values of the effective conductivity σ_{yy} in the vertical plane normal to the dip equator for longitude 80°E (for India) and for longitude 280°E (for Peru). The numbers indicated along the contours are in units of 10^{-15} e.m.u., or 10^{-4} mho/meter in m.k.s. units. With the assumption that E_y is uniform the electric current density is proportional to σ_{yy}, hence the profiles can be thought of as the current density profiles. It should be noted that the horizontal scale is 20-fold contracted; therefore, the actual profiles are much more oblong horizontally than is seen in these figures.

Electrojet over Peru (280°E)

The peak of σ_{yy} is at 103.5 km altitude directly above the dip equator, and its value is 118 in the units used in Figure 3, i.e., 1.18×10^{-13} e.m.u. (1.18×10^{-2} mho/meter). The altitudes at which σ_{yy} is reduced to one-half the peak are 97 km and 110.5 km directly above the dip equator. The contour for this half-peak value extends horizontally from 50 km north to 80 km south of the dip equator. It is noted that the electrojet profile is not symmetric with respect to the dip equator; this feature is solely due to the asymmetry of the magnetic field with respect to the dip equator.

Electrojet over India (80°E)

The σ_{yy} peak is at 102.0 km altitude above the dip equator, and its value is 71 in the same units as in Figure 2, i.e., 0.71×10^{-13} e.m.u.

(0.71×10^{-2} mho/meter). Thus over India the peak altitude is about 1.5 km lower than over Peru and the peak value over India is only 60% of that over Peru. The altitudes at which σ_{yy} is one-half the peak are 95.5 km and 110 km. Thus the thickness of the electrojet measured by these altitudes is nearly the same in India as in Peru; the thickness so defined is about 14 km. However, the steepness of the conductivity variation with height is much more pronounced over Peru than over India. Horizontally the contour for the half-peak value extends from 55 km north to 40 km south of the dip equator over India. There is a tendency that the electrojet stretches more to the south than to the north in Peru, while in India the tendency is opposite. It is noted that not only is the peak current density smaller over India than over Peru the width of the electrojet is much narrower over India. To illustrate the large differences between the profiles the contours for these longitudes are superimposed upon each other in Figure 4.

It is interesting to note that the altitude of the major part of the electrojet is a little lower than the altitude at which the normal Sq current flows at latitudes slightly off the dip equator as if the electrojet hangs below the Sq current sheet.

At other longitudes

As has been shown above for two representative longitudes the peak value of σ_{yy} over the dip equator varies considerably with longitude. The maximum of this σ_{yy} peak occurs near longitude 310°E where its value is 1.33×10^{-13} e.m.u. and the minimum near 90°E where the peak value of σ_{yy} is 0.68×10^{-13} e.m.u. Thus with regard to the σ_{yy} peak India is

close to the minimum and Peru to the maximum, making this pair well suited for further experimental studies of longitudinal inequality of the electrojet.

Having constructed conductivity profiles for different longitudes it is possible to calculate the longitudinal variation of the magnetic field produced by the model electrojet. The horizontal magnetic field ΔH_o at the dip equator due to the electrojet is shown in Figure 5 as a function of longitude; values are normalized in the manner explained below to make them comparable with the observational data. The scale can be adjusted, however, by multiplying a constant. It is noted that the value of ΔH_o at 280°E is almost twice that at 80°E.

To compare the computed field with the observations at the six magnetic observatories listed in Table 1 the horizontal component of the electrojet field at the actual locations of these observatories was computed. There will be an induction effect from the conducting earth, and this effect may be different at different observatories. However, for the sake of simplicity we assume that the horizontal component of the magnetic field due to the electrojet is increased by the induction at the same rate everywhere. Then this factor can be absorbed in the normalization constant in the computed field. For the observational data we take the peak amplitude in H measured from the midnight value for the annual average H variation for the five international quiet days for 1958. Denoting these values by the observed ΔH, the normalization constant for the calculated ΔH is determined so that the average of the latter over the six observatories becomes equal to the corresponding

average of the observed ΔH. The observed and the calculated ΔH so defined are plotted in Figure 6.

The agreement between the computed and the observed values of ΔH is only qualitative. The computed ΔH for Huancayo is too large and those of Trivandrum and Ibadan too small compared with the corresponding observed values. The longitudinal variation of ΔH calculated here seems to be much larger in amplitude than is observed. Without quantitative arguments we point out that the change in the conductivity with longitude will reduce the longitudinal variation of the electrojet intensity because of the electrostatic field set up by the electrojet itself; in particular, at longitudes near the conductivity maximum at 310°E longitude the electrojet may be appreciably suppressed by this effect. It is also pointed out that the observed values used in this paper are the annual averages of the amplitude in H and are only crude measures. The primary purpose of the present paper is to present a model profile of the electrojet, and not to discuss the longitudinal variation in the intensity of the electrojet in precise terms. Also the observed average amplitude ΔH (measured from the midnight level) has large seasonal variations. The amplitude is largest in equinox for all the stations except for Jarvis Island where it is a maximum in December solstice; while the amplitude is smallest in December solstice for Ibadan, Addis Ababa, and Trivandrum, but for Jarvis Island, Koror, and Huancayo the minimum is in June solstice. Thus it appears that factors other than the longitudinal inequality in the permanent magnetic field play an important

part in producing the longitudinal variation in the electrojet.

As to the width of the electrojet there is little observational data to compare with the present result. However, Onwumechilli (1959b) estimated the width of the electrojet in Nigeria to be about 440 km; while Forbush and Casaverde (1961) took the electrojet width to be about 660 km in Peru. Since these figures are based on different models, they cannot be compared directly. Nevertheless the tendency that the electrojet is of greater width in South America than in Africa is in complete agreement with our present results.

Magnetic field distribution through the electrojet

To provide theoretical values to be compared with the recent rocket measurements the magnetic field was computed as a function of height directly above the dip equator both for longitudes 80°E and 280°E; the results are shown in Figure 7. In the calculation the value of E_y was adjusted so as to give values of ΔH at ground level comparable with the typical observed values in India and in Peru during the periods the rocket firings were made. For 80°E, i.e., for India, the electrojet field at ground level on the dip equator is 24γ; if the induction effect is taken to be one-half of this value, the total field will be 36γ. For 280°E, i.e., for Peru, the electrojet field at the ground is taken to be 53γ so that with the same rate for the induction effect as above the total field would be about 80γ. These values are very much lower than those observed in 1958 because the solar activity is near a minimum during the period we are concerned here. In Figure 7 the magnetic

field directly due to the electrojet alone is shown without the induced field. When the induction effect is included the magnetic field gradient below 90 km would tend to become smaller than is shown in these figures.

With the present model there is a sudden reversal in the vertical gradient of the magnetic field at about 90 km altitude, above which the field change is very nearly linear to about 115 km. There is a second turning point at about 125 km to 130 km altitude, and the change becomes nearly linear again above this level.

Discussions

1. Rastogi (1962) compared the observed electrojet effects in the American, African, and Indian zones and showed that the effect is most pronounced in the American zone, less so in Africa and least in India. This is in agreement with the present result shown in Figure 5. By an approximate calculation Rastogi argued that σ_3 at 100 km level varies very little with longitude, and suggested that the observed large longitudinal variation is probably due to a longitudinal variation in the electric field. However, the present calculation shows that σ_3 varies appreciably with longitude, the ratio of σ_3 at 80°E to that at 280°E being 0.61 at 102.5 km altitude. The errors introduced by the approximations in Rastogi's argument contribute enough to mask the dependence of σ_2^2/σ_1 on the magnetic field. The wind pattern and the electron density distribution are not likely to be exactly the same along the equator, but we point out that the asymmetry of the magnetic field alone

could give rise to a considerable longitudinal variation in the electrojet intensity.

2. In the dynamo theory the conductivity is usually integrated over the thickness of the ionosphere. The integrated value of our σ_3 from 90 km to 160 km altitude is compared in Table 2 with the height-integrated σ_3 given by other workers. Although these values are in agreement in magnitude, it seems that for detailed studies of the global Sq current system the variation in the conductivity with longitude (as well as with latitude), in addition to the variations with season and solar cycle, should be taken into account. A new calculation is under way to construct an electrojet model based on the actual rocket measurement of electron density recently made over the dip equator off the coast of Peru.

3. Since the Hall current due to the vertical polarization field is the main constituent of the electrojet, the average electron velocity, v_e, can be approximately represented by

$$v_e = (E_z/B)/(1 + \nu_e^2/\omega_e^2)$$

where ν_e and ω_e are the electron collision and cyclotron frequencies respectively. The direction of the electron stream is westward. At the electrojet height $\nu_e \ll \omega_e$, and hence the average electron velocity is very nearly E_z/B. Therefore, if E_y is uniform, v_e varies with height proportionately with the ratio σ_2/σ_1. Thus when E_y/B is multiplied to the abscissa in Figure 1, it approximately gives the average drift velocity of the electrons in the electrojet as a function of height. Throughout the height range 90 km to 130 km over Peru v_e is given, to a

good approximation, by $3.8 \times 10^4 (\sigma_2/\sigma_1) E_y$ m/sec when E_y is expressed in volts/m. When $E_y = 2.4 \times 10^{-3}$ volts/m, ΔH at Huancayo due directly to the electrojet is 100γ; if the induction effect is taken to be one-half of this external field, the total variation observed will be about 150γ. With this value of E_y, the average electron drift velocity at the height of the peak current is 2.7 km/sec. The average ion velocity is little affected by the presence of the large polarization field in the electrojet, and is only of the order of a few meters per second at the most in the 100 km to 110 km region. During sunspot minimum years the average electron streaming velocity at the electrojet peak would be about one-half of the above estimate.

Farley (1963a, 1963b) and Buneman (1963) have shown that if the streaming electron velocity relative to the corresponding ion velocity exceeds the ion thermal velocity a two-stream plasma instability can occur and they attributed a certain type of E region irregularities observed at the dip equator (and in the auroral zone) to longitudinal ion waves generated by this instability. The observational aspect of this interesting phenomenon has been discussed in detail by Bowles, Balsley, and Cohen (1963) and Cohen and Bowles (1963). The ion thermal velocity in the electrojet region is about 400 m/sec. If we take this value as the minimum critical electron drift velocity for the instability, the present model over Peru shows that if E_y is taken to be 2.4×10^{-3} volts/m, the average electron drift velocity in the electrojet region is well above this critical value.

Zmuda (1960) estimated the electron drift velocity at 310 m/sec. This value is based on a current density of 1×10^{-5} amp/m^2 with an electron density of 2×10^5 electrons/cm^3. His estimate of the average electron velocity is considerably lower than our estimate. At the height of the peak current density in the present model the electron density is 8.0×10^4 electrons/cm^3, and the current density is 2.8×10^{-5} amp/m^2. As was pointed out by himself the high electron density Zmuda used corresponds to the density in a sporadic E layer; while the present electron density may be thought to be a value under a normal condition. In Zmuda's model the electric current density is averaged over the thickness of the electrojet; therefore, the current density quoted above must be considerably lower than that at the peak of the electrojet. As to the estimate of the electric field, Zmuda's estimate, 4×10^{-4} volts/m, is lower than the value adopted here, namely, 2.4×10^{-3} volts/m. This is because Zmuda took σ_3 to be constant through the electrojet region ; moreover his value of σ_3, i.e., 2.5×10^{-2} mho/m, is higher than the present estimate at the electrojet peak, i.e., 1.18×10^{-2} mho/m; his σ_3 is high because of the high electron density in his model. Matsushita (1962) estimated the horizontal electric field to be 1.6×10^{-3} volts/m, and obtained an estimate of the average electron drift velocity of 500 m/sec by averaging the current over the thickness of the electrojet. Since these authors assumed the current to be uniform over a thickness of a few tens km, the current density is greatly reduced compared with the present current density estimate for the peak electrojet altitude.

Acknowledgements

We wish to thank Dr. S. J. Bauer for providing the data for the electron density profile and Dr. N. C. Maynard for giving information on the magnetic field observations on the ground in India and in Peru at the time the University of New Hampshire rocket firings were made.

APPENDIX

The conductivity elements σ_o, σ_1, and σ_2 (in e.m.u.) are calculated by the following formulas:

$$\sigma_o = N_e\, e^2\, [(m_e\nu_e)^{-1} + (m_i\nu_i)^{-1}]$$

$$\sigma_1 = N_e\, e^2\, [(m_e\nu_e)^{-1}\, \nu_e^2(\nu_e^2 + \omega_e^2)^{-1} + (m_i\nu_i)^{-1}\, \nu_i^2(\nu_i^2 + \omega_i^2)^{-1}]$$

$$\sigma_2 = N_e\, e^2\, [(m_e\nu_e)^{-1}\, \nu_e\omega_e(\nu_e^2 + \omega_e^2)^{-1} - (m_i\nu_i)^{-1}\, \nu_i\omega_i\, (\nu_i^2 + \omega_i^2)^{-1}]$$

where

N_e = electron density, electrons/cm^3

e = magnitude of the electronic charge

$m_{e,i}$ = electron, or ion, mass

$\nu_{e,i}$ = electron, or ion, collision frequency

$\omega_{e,i}$ = electron, or ion, cyclotron frequency, taken to be positive regardless of the sign of charge

It is assumed that there is only one type of singly ionized ions.

Because of the polarization of the medium the electron density is not exactly the same as the ion density. However, the deviation (ΔN_e) from the neutrality is extremely small. Assuming that all the quantities concerned vary with z alone, we can estimate the charge density from Poisson's equation: $dE_z/dz = 4\pi c^2 e\Delta N_e$.

Thus

$$\Delta N_e = (4\pi c^2 e)^{-1}\, E_y\, d(\sigma_2/\sigma_1)/dZ$$

Taking $E_y = 2.4 \times 10^3$ e.m.u., ΔN_e is of the order of 10^{-4} cm^{-3} in the electrojet region. Thus the assumption of neutrality in the computation of the conductivity elements is justified.

Following Chapman (1956) the collision frequencies are computed by the following formulas:

$$\nu_e = \nu_{ei} + \nu_{en}$$

where

$$\nu_{ei} = [34 + 4.18 \log (T^3 N_e^{-1})] N_e T^{-3/2}$$

$$\nu_{en} = 5.4 \times 10^{-10} N_n T^{1/2}$$

and

$$\nu_i = \nu_{in} = 2.6 \times 10^{-9} (N_e + N_n) W^{-1/2}$$

where N_n, T, and W are the neutral particle density, the temperature, and the mean molecular weight of the ions (which is assumed to be equal to that of the neutral particles).

The atmospheric model given by Champion and Minzner (1963) was used for N_n, T, and W. These data together with the computed collision frequencies are given in Table 3 in an abbreviated form. The profile of the electron density N_e used is shown by the heavy curve in Figure 8; this curve is a smoothed average of the two dotted curves that represent the rocket data obtained at Wallops Island by Bauer and Jackson (1963) with the CW propagation technique. The electron density profile adopted here is meant only to serve as a model. In a new model to be presented in a later publication the electron density determined by the actual rocket measurements in the electrojet region and a more recently determined spherical harmonic representation of the main field will be used.

References

Baker, W. G., and D. F. Martyn, Electric currents in the ionosphere, I. The conductivity, Phil. Trans. Roy. Soc. London A, 246, 281-294, 1953.

Bauer, S. J., and J. E. Jackson, A small multi-purpose rocket payload for ionospheric studies, NASA Technical Notes TN-D2323, 1963.

Bowles, K. L., B. B. Balsley, and R. Cohen, Field-aligned E-region irregularities identified with acoustic plasma waves, J. Geophys. Res., 68, 2485-2501, 1963.

Buneman, O., Excitation of field aligned sound waves by electron streams, Phys. Rev. Letters, 10, 285-287, 1963.

Champion, K. S. W., and R. A. Minzner, Revision of United States Standard Atmosphere 90 to 700 kilometers, Rev. Geophys., 1, 57-84, 1963.

Chapman, S., The electrical conductivity of the ionosphere: a review, Nuovo Cimento, Supp. No. 4, 4, Ser. X, 1385-1412, 1956.

Cohen, R., and K. L. Bowles, The association of plane-wave electron-density irregularities with the equatorial electrojet, J. Geophys. Res., 68, 2503-2525, 1963.

Davis, T. N., K. Burrows, and J. D. Stolarik, A low latitude survey of the equatorial electrojet with rocket-borne magnetometers, presented at the Second Conference on Direct Aeronomic Measurements in the Lower Ionosphere, Urbana, Illinois, 1965.

Farley, Jr., D. T., Two-stream plasma instability as a source of irregularities in the ionosphere, Phys. Rev. Letters, 10, 279-282, 1963a.

Farley, Jr., D. T., A plasma instability resulting in field-aligned irregularities in the ionosphere, J. Geophys. Res., 68, 6083-6097, 1963b.

Fejer, J. A., Semidiurnal currents and electron drifts in the ionosphere, J. Atmos. Terr. Phys., 4, 184-203, 1953.

Forbush, S. E., and M. Casaverde, Equatorial electrojet in Peru, Carnegie Inst. Wash. Publ. 620, Wash., D.C., 1961.

Hendricks, S. J., and J. C. Cain, Magnetic Field Data for Trapped Particle Evaluations, J. Geophys. Res., to be published in the Jan. 1, 1966 issue.

Hirono, M., A theory of diurnal magnetic variations in equatorial regions and conductivity of the ionosphere E region, J. Geomag. Geoelec., 4, 7-21, 1952.

Hirono, M., and Kitamura, T., A dynamo theory in the ionosphere, J. Geomag. Geoelec., 8, 9-23, 1956.

Jensen, D. C., and J. C. Cain, An interim geomagnetic field, (Abstract), J. Geophys. Res., 67, 3568-3569, 1962.

Maeda, H., The vertical distribution of electrical conductivity in the upper atmosphere, J. Geomag. Geoelec., 5, 94-104, 1953.

Maeda, H., Horizontal wind systems in the ionospheric E region deduced from the dynamo theory of the geomagnetic Sq variation, Part I. Non-rotating earth, J. Geomag. Geoelec., 7, 121-132, 1955.

Matsushita, S., Interrelations of sporadic E and ionospheric currents, pp. 344-375, Ionospheric Sporadic E, edited by E. K. Smith, Jr., and S. Matsushita, MacMillan Co., New York, 1962.

Maynard, N. C., and L. J. Cahill, Jr., Measurement of the equatorial electrojet in India, to be published in J. Geophys. Res., 1965a.

Maynard, N. C., and L. J. Cahill, Jr., Preliminary results of measurements of Sq currents and the equatorial electrojet near Peru, to be published in J. Geophys. Res., 1965b.

Onwumechilli, C. A., A study of the equatorial electrojet, I. An experimental study, J. Atmos. Terr. Phys., 13, 222-234, 1959a.

Onwumechilli, C. A., A study of the equatorial electrojet, II. A model electrojet that fits H-observations, J. Atmos. Terr. Phys., 13, 235-257, 1959b.

Osborne, D. G., Equatorial electrojet in Ghana, Nature, 193, 567-568, 1962a.

Osborne, D. G., Position and movement of the equatorial electrojet over Ghana, J. Atmos. Terr. Phys., 24, 491-502, 1962b.

Osborne, D. G., Daily variability in strength of the equatorial electrojet, 68, 2435-2439, 1963.

Price, A. T., and G. A. Wilkins, New methods for the analysis of geomagnetic fields and their application to the Sq field of 1932-3, Phil. Trans. Roy. Soc. London A, 256, 31-98, 1963.

Rastogi, R. G., Longitudinal variation in the equatorial electrojet, J. Atmos. Terr. Phys., 24, 1031-1040, 1962.

Zmuda, A. J., Ionospheric electrostatic fields and the equatorial electrojet, J. Geophys. Res., 65, 2247-2253, 1960.

Table 1. Six equatorial observatories used in this paper.

Observatory	Longitude	Latitude	Dip*	Distance from dip equator to station**
Ibadan	3.°90E	7.°43N	-5.°29	233km
Addis Ababa	38.77E	9.03N	-1.42	56
Trivandrum	76.95E	8.50N	-1.94	83
Koror	134.50E	7.33N	-0.22	21
Jarvis Island	160.03W	0.38S	1.77	-80
Huancayo	75.33W	12.05S	0.70	-48

* Computed values based on the spherical harmonic representation of the main field, and not observed values.

** The distance between the computed dip equator and the station; positive when the station is south of the dip equator.

Table 2. Comparison of estimates of the height-integrated σ_3 by several workers.

Present paper	80°E	1.21 x 10^{-7} e.m.u.
	280°E	1.97
H. Maeda (1953)		0.775
Baker and Martyn (1953)		1.64
Fejer (1953)		1.80
Chapman (1956)	hot ionosphere	2.08
	cold ionosphere	1.93
Hirono and Kitamura (1956)		1.52

Table 3. The atmospheric model used in this paper.

Height	N_n	W	T	ν_e	ν_i
	cm^{-3}		^oK	sec^{-1}	sec^{-1}
90 km	6.584×10^{13}	29.00	180	4.77×10^5	3.18×10^4
100	1.036×10^{13}	28.88	210	7.61×10^4	5.02×10^3
110	2.073×10^{12}	28.56	257	1.63×10^4	1.01×10^3
120	5.235×10^{11}	28.07	349	4.72×10^3	2.57×10^2
130	1.650×10^{11}	27.70	515	1.85×10^3	8.15×10^1
140	7.476×10^{10}	27.31	715	1.03×10^3	3.72×10^1
150	4.115×10^{10}	26.93	893	7.22×10^2	2.06×10^1
160	2.622×10^{10}	26.65	1022	5.89×10^2	1.32×10^1

Figures

Figure 1. The ratio σ_2/σ_1 (for 280°E longitude) as a function of height.

Figure 2. The conductivity (σ_{yy}) profile for longitude 80°E for India in the vertical plane perpendicular to the dip equator; contours of equal σ_{yy} are drawn in units of 10^{-15} e.m.u., or 10^{-4} mho/meter; north to the right. Note that the horizontal scale is 20-fold contracted in comparison with the vertical scale.

Figure 3. The conductivity (σ_{yy}) profile for longitude 280°E for Peru, units are the same as in Figure 2.

Figure 4. A comparison of the conductivity profiles for longitudes 80°E and 280°E; units are the same as in Figures 2 and 3.

Figure 5. The computed electrojet field at the dip equator as a function of longitude.

Figure 6. Comparison of the observed values of ΔH with those computed, for six equatorial observatories.

Figure 7. The magnetic field produced by the electrojet as a function of height, for longitudes 80°E and 280°E.

Figure 8. The electron density profile used in this paper. Two curves drawn with broken lines represent profiles obtained by rockets over Wallops Island (Bauer and Jackson, 1963).

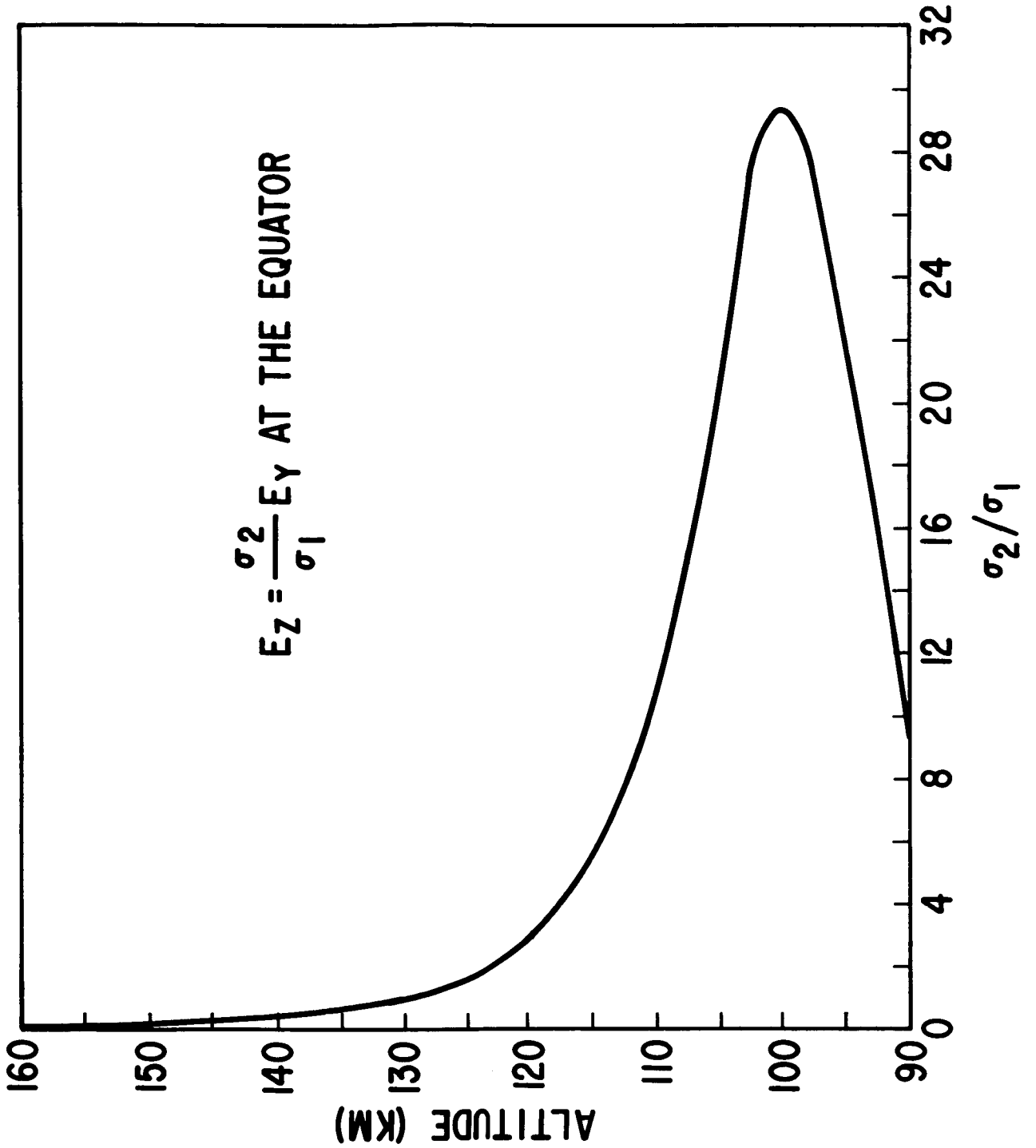
$E_Z = \frac{\sigma_2}{\sigma_1} E_Y$ AT THE EQUATOR
ALTITUDE (KM)
160
150
140
130
120
110
100
90
0
4
8
12
16
20
24
28
32
σ_2/σ_1

Figure 1

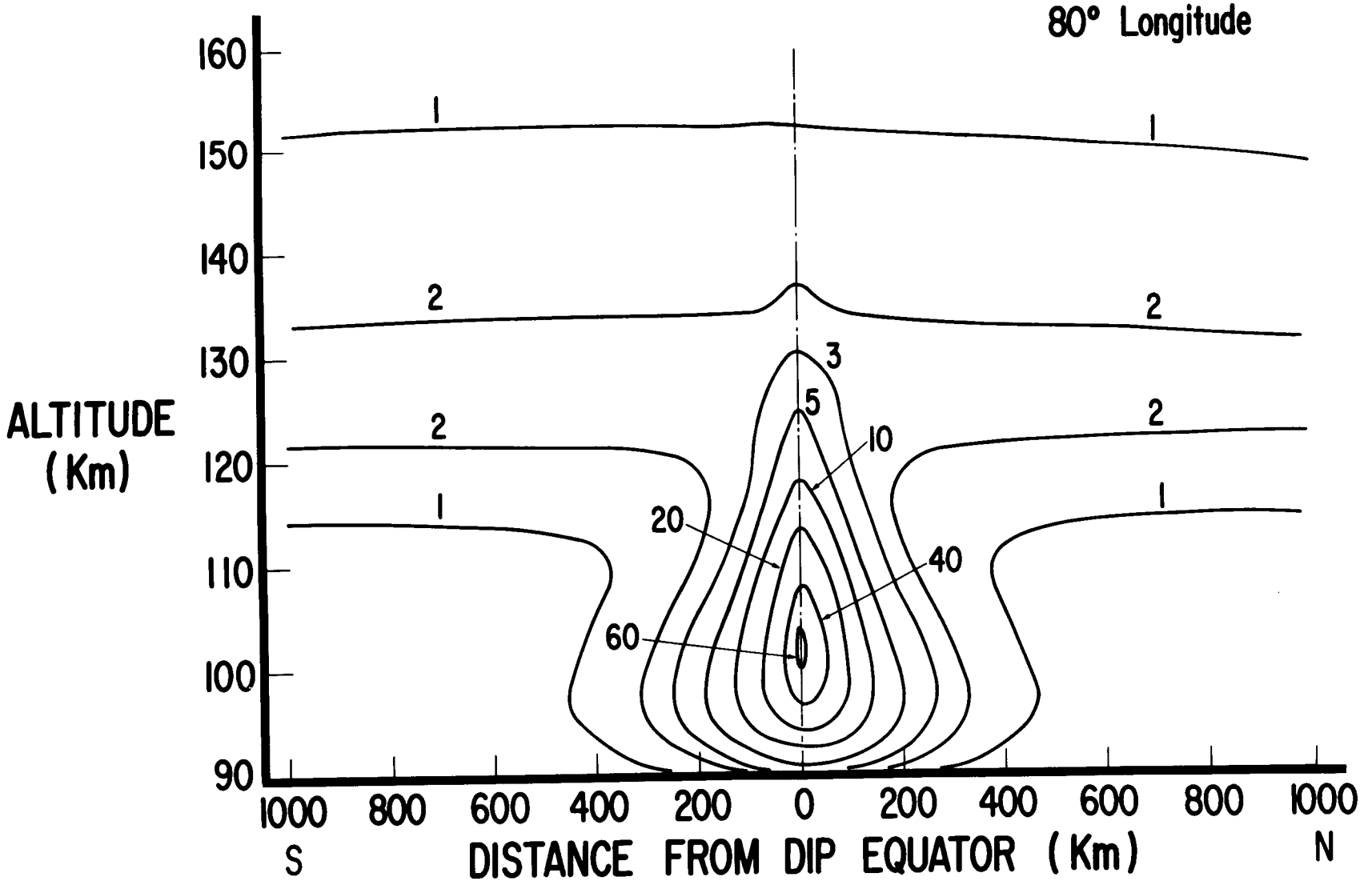
80° Longitude
ALTITUDE
(Km)
160
150
140
130
120
110
100
90
1
1
2
2
3
5
10
20
40
60
2
2
1
1000
800
600
400
200
0
200
400
600
800
1000
S
DISTANCE FROM DIP EQUATOR (Km)
N

Figure 2

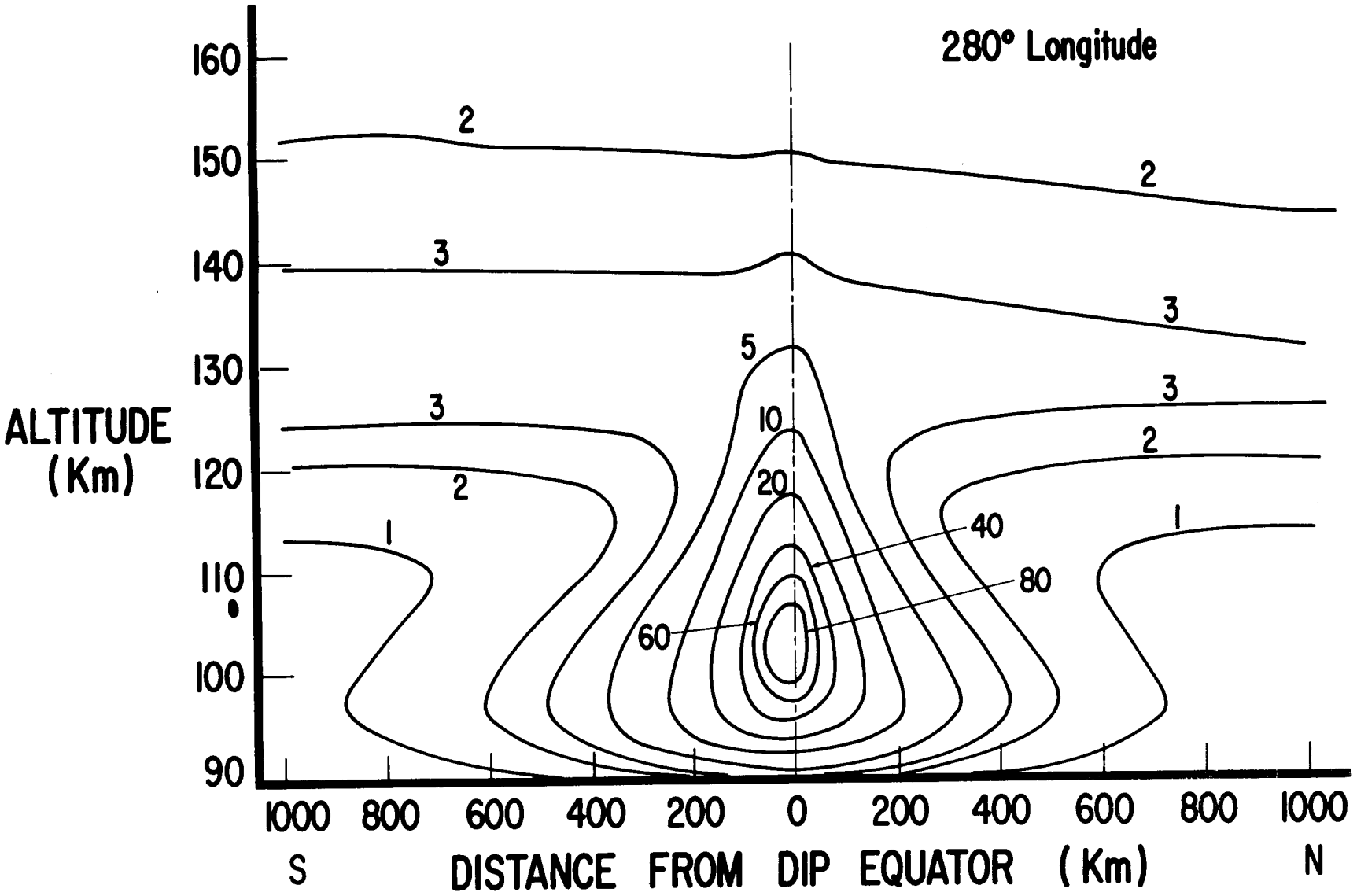
280° Longitude
ALTITUDE (Km)
160
150
140
130
120
110
100
90
2
2
3
3
5
3
10
3
2
20
2
1
40
1
80
60
1000 800 600 400 200 0 200 400 600 800 1000
S
DISTANCE FROM DIP EQUATOR (Km)
N

Figure 3

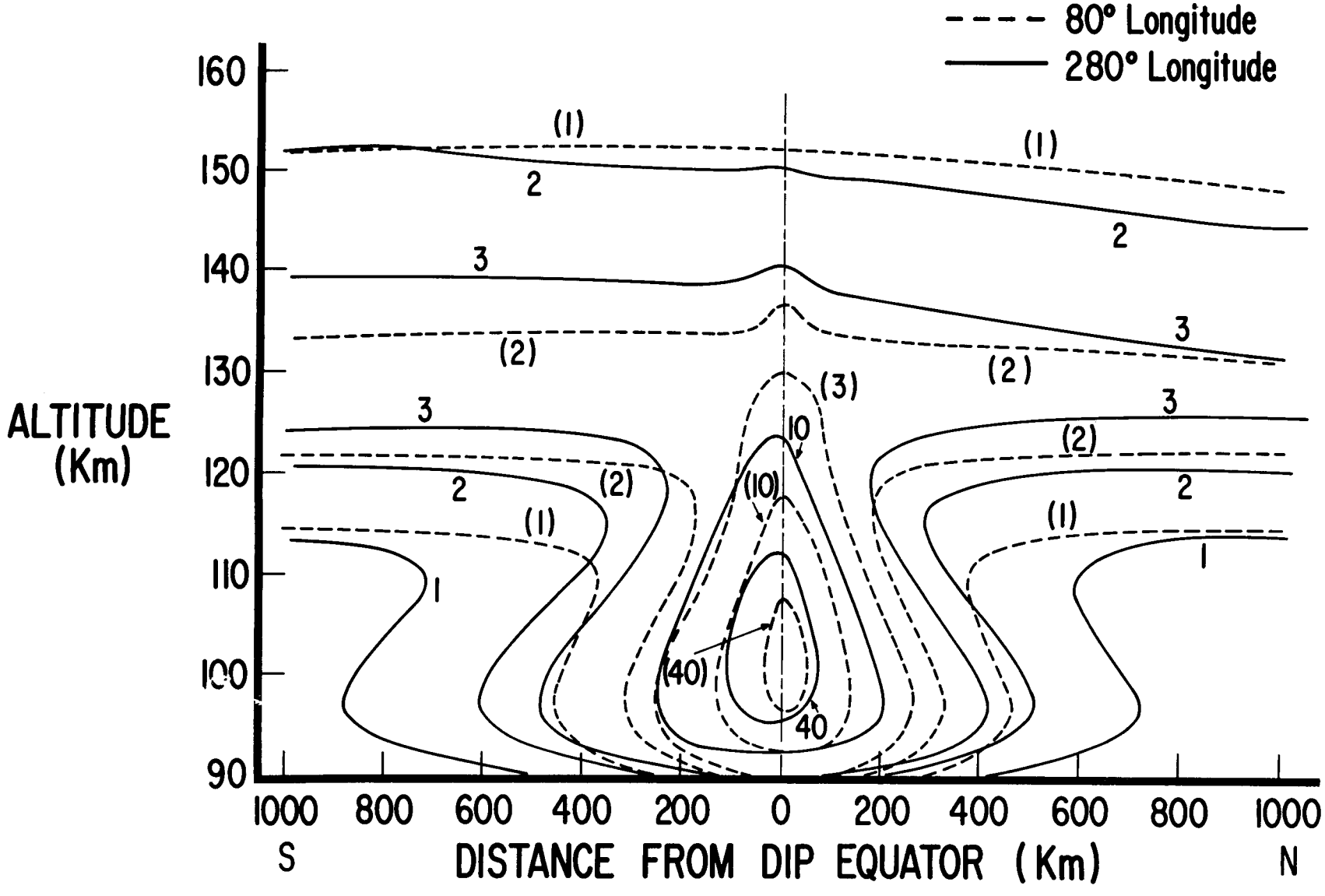
80° Longitude
280° Longitude
ALTITUDE (Km)
160
150
140
130
120
110
100
90
1000
800
600
400
200
0
200
400
600
800
1000
S
DISTANCE FROM DIP EQUATOR (Km)
N
(1)
2
3
(2)
(3)
10
(10)
(40)
40
1

Figure 4

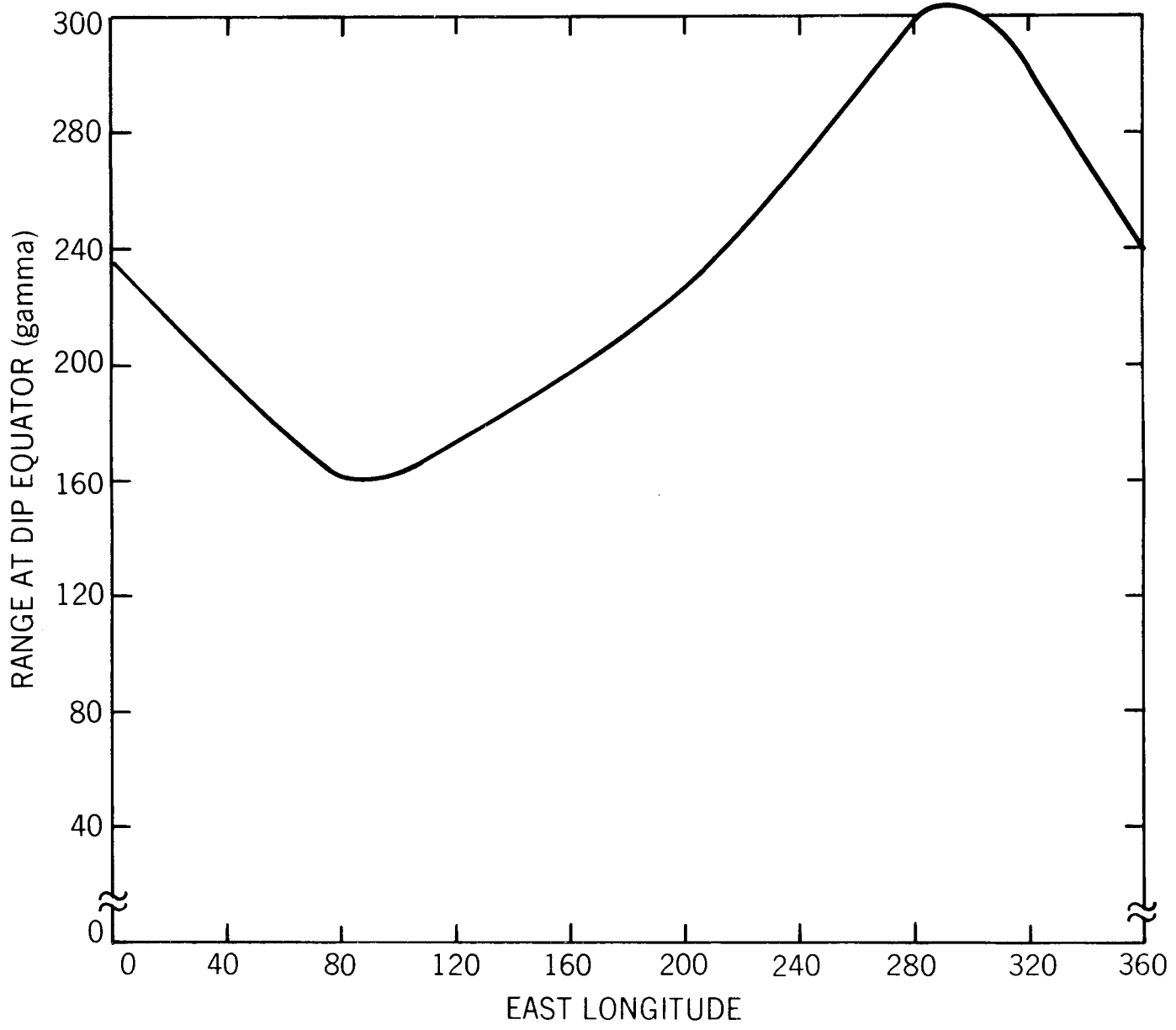
300
280
240
200
160
120
80
40
0
RANGE AT DIP EQUATOR (gamma)
0
40
80
120
160
200
240
280
320
360
EAST LONGITUDE

Figure 5

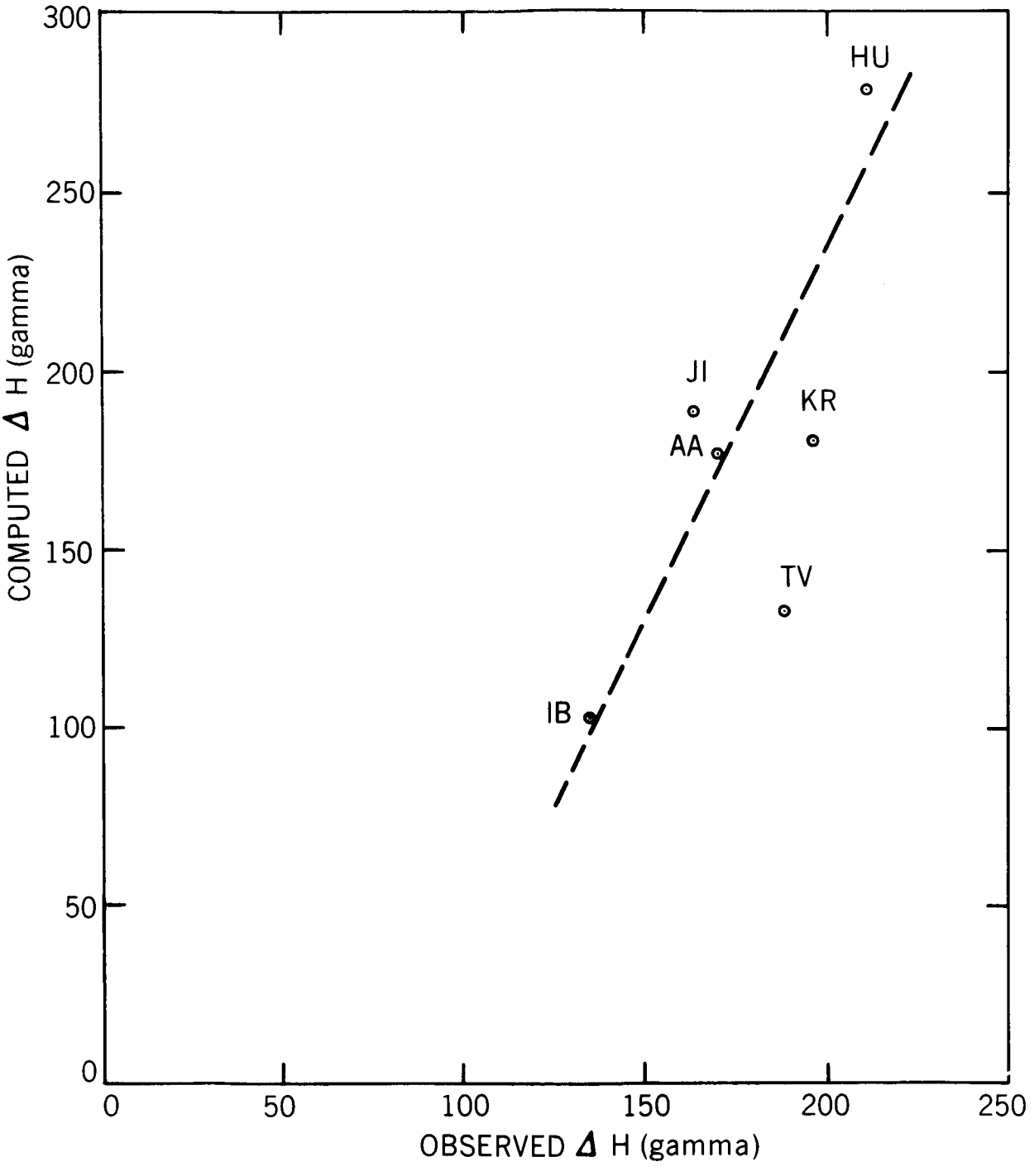
300
250
200
150
100
50
0
0
50
100
150
200
250
COMPUTED Δ H (gamma)
OBSERVED Δ H (gamma)
HU
JI
KR
AA
TV
IB

Figure 6

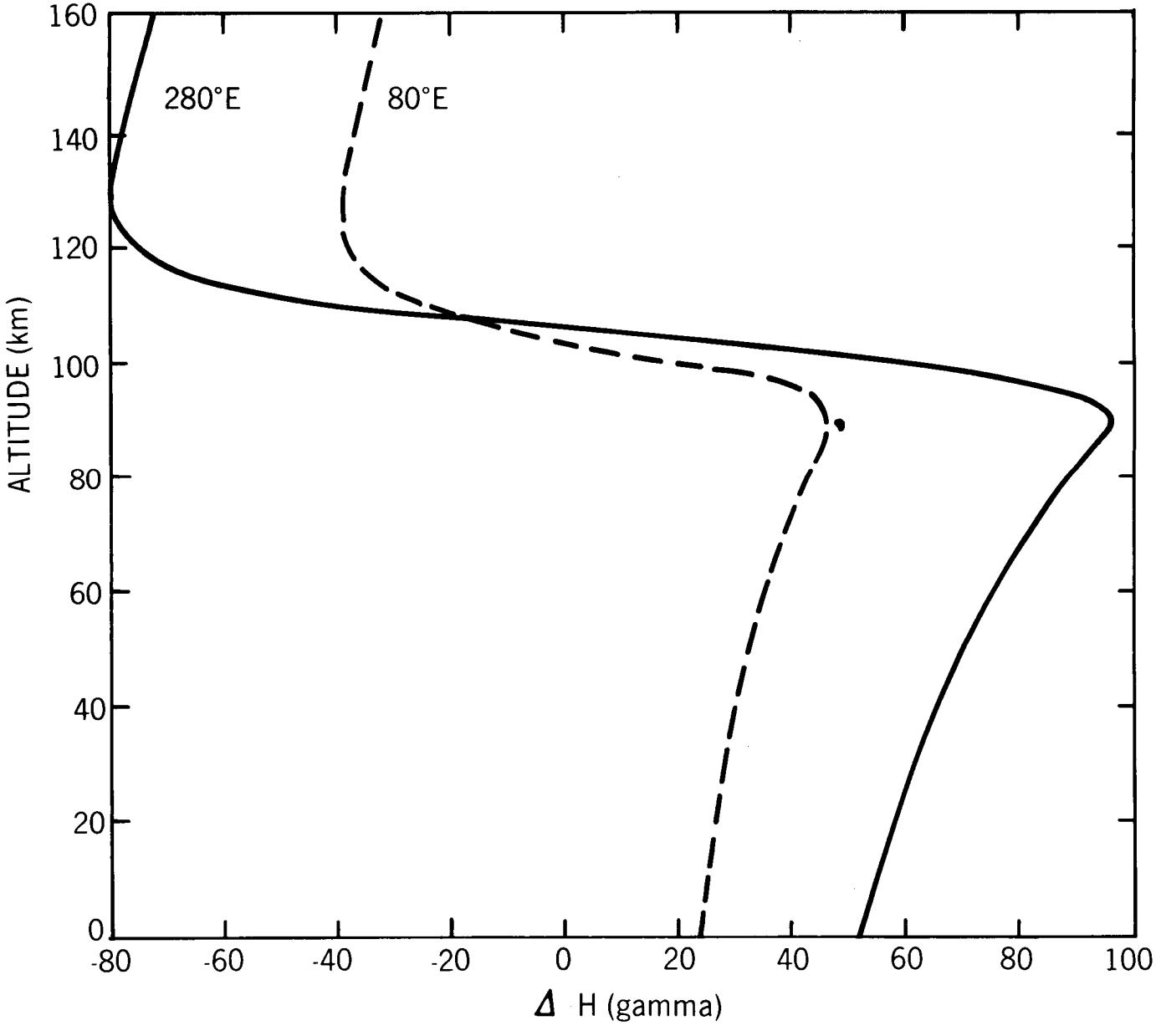
160
140
120
100
80
60
40
20
0
ALTITUDE (km)
280°E
80°E
-80
-60
-40
-20
0
20
40
60
80
100
Δ H (gamma)

Figure 7

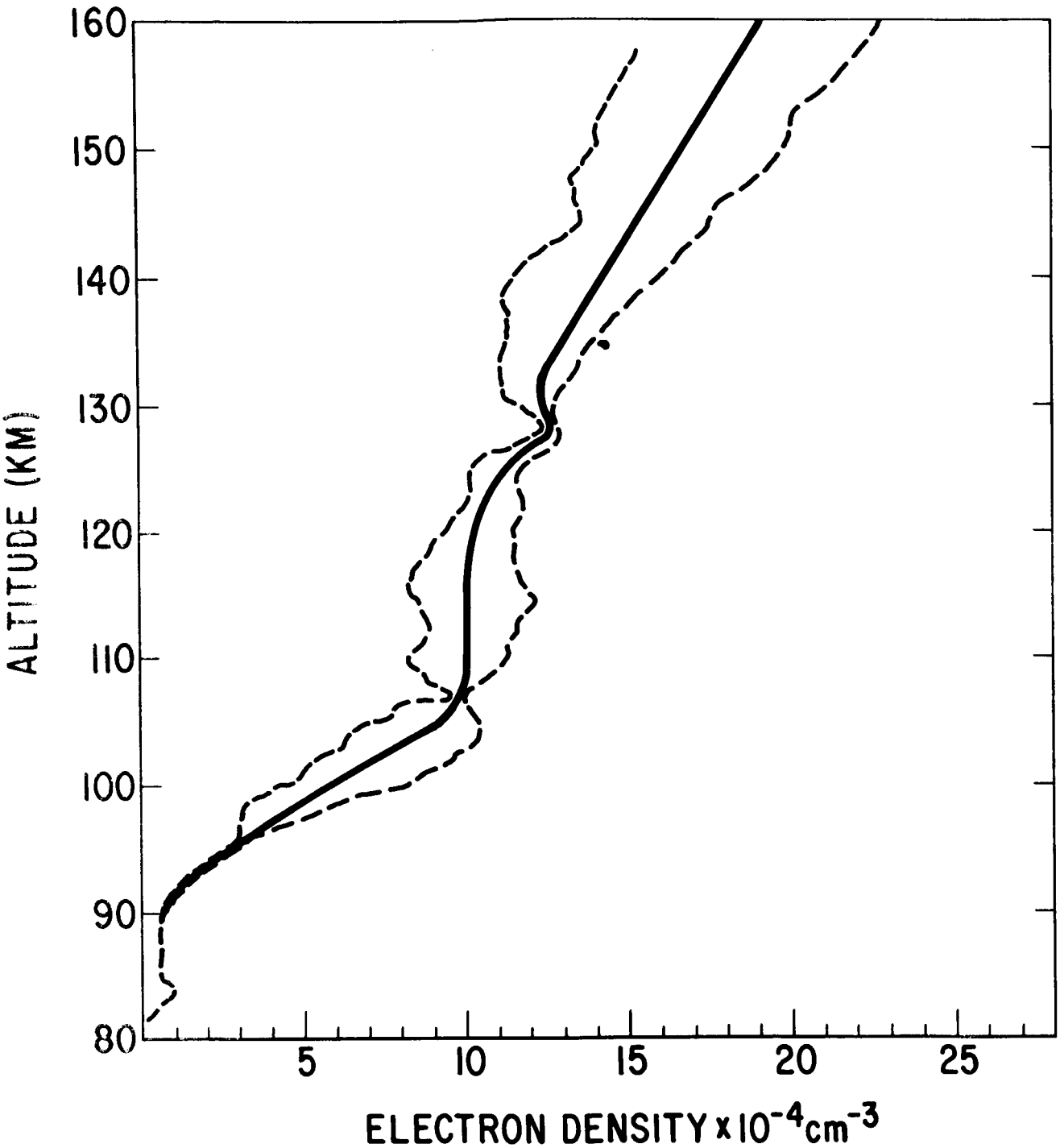
160
150
140
130
120
110
100
90
80
ALTITUDE (KM)
5
10
15
20
25
ELECTRON DENSITY x 10⁻⁴cm⁻³

Figure 8